

Optimization of Activated Carbon Production from Eucalyptus Wood Using

H₃PO₄ as the Activating Agent

ສປາວະທີ່ເໜີມສົມໃນການພົລືຕ່ານກົມມັນຕໍ່ຈາກເຄີຍໄມ້ຢູ່ຄາລີປັດສໂດຍການໃຊ້ ກຣດົຟົກໂອສົກເປັນສາງກະຕຸ້ນ

Kanokwan Seerod (กนกวรรณ ศีรอด)^{1*} Dr. Varinrumpai Seithantanabutara (ดร. วรินร์พาย เศรษฐ์ชนบุตร)**

(Received: October 5, 2018; Revised: November 1, 2018; Accepted: November 5, 2018)

ABSTRACT

Activated carbons were prepared from eucalyptus wood residue via chemical activation with H_3PO_4 as a chemical activating agent. MINITAB (version 16) software was used for investigation the effects of acid concentration (0.5-2 M), carbonizing temperature (500-700°C) and carbonizing time (60-120 min) on specific surface area. Variance analysis and RSM technique were applied to describe the polynomial model as a function of experimental parameters and its significant parameter. Model with multiple correlation coefficients of determination R^2 and R_{adj}^2 of 0.9725 and 0.9230, respectively, was proposed. Acid concentration was the most significant factor that influenced on the specific surface area. AC with high specific surface area of $365.254\text{ m}^2/\text{g}$ was obtained at the optimum condition; 2M of H_3PO_4 , 700°C and 120 min. Extra investigation at this condition was done by using smaller precursor impregnated in stronger H_3PO_4 concentration of 8M. It was found that the activated carbon AC with developing mesoporosity and improved surface area of $812.84\text{ m}^2/\text{g}$ was produced. The physical and structural properties of activated carbons were characterized by TGA, SEM and FTIR. Also their porous structures were determined by adsorption/desorption of N_2 at 77 K.

บทคัดย่อ

ถ่านกัมมันต์จากเศษไม้สูญค่าปลดสกุลเหรียญ โดยวิธีการกระตุ้นทางเคมีด้วยตัวกระตุ้นกรดฟอสฟอริก จากการเติมถ่านกัมมันต์จะมีการศึกษาปัจจัยที่ส่งผลต่อพื้นที่ผิวจำเพาะด้านโปรแกรม MINITAB (version 16) ปัจจัยที่ใช้ในการศึกษานี้ 3 ปัจจัย ได้แก่ ความชื้นขั้นของกรดฟอสฟอริก (0.5 – 2 โมลาร์) อุณหภูมิในการการรื้อปูนซีซี (500 – 700 องศาเซลเซียส) และเวลาในการการรื้อปูนซีซี (60 – 120 นาที) การวิเคราะห์ความแปรปรวนและวิธีการพื้นผิวดอนสนองจะถูกใช้ในการอธิบายสมการ โพลีโนมิลที่เป็นฟังก์ชันของตัวแปรจากการทดลองและตัวแปรที่มีนัยสำคัญ แบบจำลองสัมประสิทธิ์ทางสัมพันธ์พหุคุณที่ได้จะให้ค่าสัมประสิทธิ์แสดงการตัดสินใจ และสัมประสิทธิ์การตัดสินใจที่ปรับแก้เท่ากับ 0.9725 และ 0.9230 ตามลำดับ พบว่า ความชื้นของกรดฟอสฟอริกเป็นปัจจัยหลักที่มีอิทธิพลต่อพื้นที่ผิวจำเพาะมากที่สุดอย่างมีนัยสำคัญ ถ่านกัมมันต์ที่ให้มีค่าพื้นที่ผิวจำเพาะสูงสุดเป็น 365.254 ตารางเมตรต่อกรัม ซึ่งจะต้องหักห้ามส่วนที่ไม่สามารถดูดซึมน้ำได้ คือความชื้นขั้นของกรดฟอสฟอริก 2 โมลาร์ อุณหภูมิในการการรื้อปูนซีซี 700 องศาเซลเซียส และเวลาในการการรื้อปูนซีซี 120 นาที จากการตรวจสอบเพิ่มเติมที่สภาวะที่เหมาะสม โดยการใช้สารตั้งต้นที่มีนิยามเดลกงผ่านการปรับสภาพด้วยกรดฟอสฟอริกที่มีความชื้นขั้นสูงสุดเป็น 8 โมลาร์ จะทำให้ได้ถ่านกัมมันต์ที่มีโครงสร้างส่วนใหญ่เป็นรูพรุนขนาดกลางเพิ่มขึ้นและมีพื้นที่ผิวจำเพาะสูงสุดเป็น 812.24 ตารางเมตรต่อกรัม คุณสมบัติค้านกายภาพและโครงสร้างสารประกอบของถ่านกัมมันต์จะถูกวิเคราะห์ด้วยเครื่อง TGA SEM และ FTIR โครงสร้างรูพรุนของถ่านกัมมันต์จะถูกตรวจสอบด้วยวิธีการคุณซัมและคาบชั้นก้าวไนโตรเจนที่ 77 K

Keywords: Activated carbon, Phosphoric acid, Response surface methodology

คำสำคัญ: ถ่านกัมมันต์ กรดฟอสฟอริก วิธีการพื้นผิวตบสนอง

¹Correspondent author: tmailka@kku.ac.th

* Student, Master of Engineering Program in Chemical Engineering, Department of Chemical Engineering, Faculty of Engineering,

Khon Kaen University, Thailand

*** Assistant Professor, Department of Chemical Engineering, Faculty of Engineering, Khon Kaen University, Thailand*



Introduction

Activated carbon (AC) is a porous carbonaceous material with the highly developed surface area and rich surface groups. It is widely used as adsorbent, catalyst and catalyst support, gas separation and storage, solvent recovery and decolorizing, super capacitors, and as electrodes. The textural and chemical properties of AC are affected by many variables such as the nature of raw materials, the activation method, the activating agent and the conditions of activation process [1]. In recent years, ACs have been prepared from several agriculture and forestry wastes like cotton stalks, rice husk, corn cobs, sugar cane bagasse, palm shell, sunflower seed and cotton stalk. Eucalyptus wood, fast growing tree and abundantly available in Thailand, has a reasonably high content of carbon as starting material for the production of activated carbon. Activated carbon can be produced via two techniques; physical activation and chemical activation. Physical activation is a dual-stage mechanism that includes carbonization process under an inert atmosphere at low temperature followed by activation under the oxidizing gas atmosphere such as steam, CO_2 , binary mixture of CO_2 and N_2 or air at high temperature. But chemical activation starts with an impregnation step using chemical activating agents such as zinc chloride (ZnCl_2), potassium hydroxide (KOH) and phosphoric acid (H_3PO_4), prior to heat treatment in an inert atmosphere [2]. These dehydrating agents inhibit the tar formation during carbonization so the yield of porous carbon can be enhanced within the shorter activation time at lower activation temperature. Furthermore, the produced activated carbon presents improved surface area and well-developed pore structure. Therefore the chemical activation is more economically viable than physical activation. Mostly, phosphoric acid is the most preferable chemical activating agents due to environmental issues and economic concerns. Phosphoric acid allows the developing of both micropores and mesopores in the produced activated carbon [3].

Response surface methodology (RSM) is a collection of mathematical and statistical experimental design techniques for experimental design, model building and problem analysis. It is useful for understanding the interactions among the parameters of two or more variables that have been optimized and searching for the optimum conditions. Experiment time can be minimized because low number of experiments is required in optimization process. The two most common designs used in RSM are Central Composite Design (CCD) and Box-Behnken design (BBD). BBD is considered as an efficient option in RSM and an ideal alternative to CCD. Optimization of experimental conditions using RSM has widely applied in various processes, however, a few of applying RSM in AC preparation was found in previous reports. The major objective of this paper is to optimize the factors on AC production from eucalyptus wood. The effects of three influencing variables (i.e., H_3PO_4 concentration, carbonizing temperature and time) on the response of specific surface area of obtained AC were investigated. The textural, porous and structural properties of the prepared activated carbons were characterized.

Methodology

Eucalyptus wood (*E. camaldulensis*) was collected from local wood factory in Khonkaen province of Thailand. It was repeatedly washed with distilled water subsequently dried in an oven at 105°C for 24 h. The dried raw materials were crushed by hammer mill to obtain the size of 2-3 cm in length. Ortho-phosphoric acid of



analytical grade (H_3PO_4 , mass fraction 85% and 1.69 g/ml) was obtained from Ajax Finechem Pty Limited, Australia. All solutions were prepared in distilled water.

Preparation of activated carbon

Preparation of activated carbon from eucalyptus wood was carried out using H_3PO_4 as an activating agent. Prepared material was impregnated into different concentrations of H_3PO_4 solution (0.5-2 M) with a constant ratio as 20 g of eucalyptus wood to 170 ml of H_3PO_4 solution. The mixture was stirring for 24 h at the room temperature. Consequently the impregnated samples were separated and then dried overnight in the hot oven. The weighed sample was heated in an electrical furnace at $3^\circ C/min$ in nitrogen flow of $20\text{ cm}^3/min$. Carbonization has been carried out for 60 to 120 min at the final temperature ranging from 500 to $700^\circ C$. After completed, the cooled sample was weighed in order to determine the conversion yield. The obtained product was washed several times with warm distilled water until neutral before drying at $105^\circ C$.

Experimental design and optimization study

Box-Behnken design (BBD) with 3 factors and 3 levels was employed to the statistical optimization for the production of activated carbon from eucalyptus wood. The experimental data was analyzed using the statistical software MINITAB (version 16) to develop the polynomial regression model for determining the optimum condition. Based on the preliminary experiments, three critical parameters; H_3PO_4 concentration, carbonizing temperature and carbonizing time were selected as the independent variables affecting on the specific surface area (Y) which considered as the dependent variable (response). The experimental range and the levels of these variables are given in Table 1. The RSM was applied to optimize the experimental conditions for the production of AC with high specific surface area. To correlate the dependent and independent variables, the experimental data was analyzed by the response surface regression procedure to fit the following second-order polynomial response equation (1), providing regression coefficients.

$$Y = \beta_0 + \beta_1 X_1 + \beta_2 X_2 + \beta_3 X_3 + \beta_{12} X_1 X_2 + \beta_{13} X_1 X_3 + \beta_{23} X_2 X_3 + \beta_{11} X_1^2 + \beta_{22} X_2^2 + \beta_{33} X_3^2 + \varepsilon \quad (1)$$

Where Y is the response and X_1 , X_2 and X_3 are the independent variable effects. X_1^2 , X_2^2 and X_3^2 are the square effects. X_{12} , X_{13} and X_{23} are the interaction effects. β_1 , β_2 and β_3 are the linear coefficients. β_{11} , β_{22} and β_{33} are the squared coefficients. β_{12} , β_{13} and β_{23} are the interaction coefficients. β_0 and ε is the constant and the random error, respectively. There were 15 experiments performing in this study. The interaction between the variables and the response was found out by analysis of variance (ANOVA) based on the proposed model. The quality of the fit of the regression model was expressed with the coefficient of determination (R^2 , R_{adj}^2), and statistical significance was checked by the F-test. Model terms were selected or rejected based on the probability value with 95% confident level. Finally, 3D response surfaces were drawn to visualize the individual and interactive effects of the independent variables on the AC surface area.



Characterization of the activated carbons

Basic functional groups of prepared AC samples were analyzed by Fourier Transform Infrared Spectroscopy (FTIR, S5_iD5, Thermo Scientific Nicolet), record from a wavenumber in the region of 400-4000 cm^{-1} . AC sample was ground to a particle size less than 80 mesh and dried at 150 $^{\circ}\text{C}$ for 3h prior to analysis. The surface morphology revealing porous texture of char and AC samples was observed under Scanning Electron Microscope (SEM, S-3000N, HITACHI). The resolution was 5 nm in variable pressure mode with an accelerating voltage between 0.3-30 kV. As the samples were not electrically conductive, they were gold plated before observation. The specific surface area and porous characteristics of the AC samples were determined by N_2 adsorption/desorption at 77K using Micromeritics ASAP 2010. The sample was degassed at 200 $^{\circ}\text{C}$ under vacuum for 6 h prior to measurement. The BET specific surface area (S_{BET}) of AC was estimated from N_2 adsorption isotherm based on Brunauer Emmet and Teller (BET) equation by applying relative pressure in the range of 0.001-0.3 bar. The micropore surface area (S_{mi}) and the volume of micropores (V_{mi}) were obtained from t-plot micropore area and t-plot micropore volume, respectively. The mesopore surface area (S_{me}) was determined by subtracting S_{mi} from S_{BET} . The total pore volume (V_{T}) was estimated from the amount of N_2 adsorbed at relative high pressure ($P/P_0 \sim 0.99$). The mesopore volume (V_{me}) was calculated by subtracting V_{mi} from V_{T} . The pore size distribution of prepared AC sample was determined according to BJH (Barrett-Joyner-Halenda) model. The elemental analysis of the raw materials was carried out in a CHNS/O Analyzer, Thermo Quest Flash EA 1112 Series. The proximate analysis and thermal stabilities of eucalyptus wood, char and derived-ACs were analyzed using a thermogravimetric analyzer (TGA, 50-Shimadzu Japan). The weight loss of sample was automatically monitored continuously as a function of the heating time and temperature. The rate of weight loss as a function of time was derived from TGA curve resulting in a derivative TG curve.

Results

Properties and thermal decomposition of Eucalyptus wood

From the proximate and ultimate analysis of the Eucalyptus wood (*E. camaldulensis*) as shown in Table 2, eucalyptus wood contained moisture content of 5.64wt.%. The dried wood had fixed carbon, volatile matter and ash content of 16.61, 82.41 and 0.98wt.%, respectively. Eucalyptus wood contained carbon, hydrogen, nitrogen and oxygen (calculated by difference) of 52.4, 0.3, 5.1 and 42.2wt.%, respectively. Therefore, eucalyptus wood was taken into account in this study because of its relatively high content of fixed carbon and carbon element, high proportion of volatile matter and low ash content.

Optimization of activated carbon process

1. Fitting model and analysis of variance

The MINITAB (version 16) software was used for statistical analysis to evaluate the preparation of activated carbon from eucalyptus wood. The polynomial regression equation was developed based on BBD in order to analyze factor interactions contributing to the regression model and to determine the optimum values. The H_3PO_4 concentration, carbonizing temperature and carbonizing time for the production of activated carbons were optimized



based on the specific surface area of those produced ACs. The design of experiments runs is given in Table 3, together with the corresponding experimental results. The yield of the activated carbon was defined as the ratio of the weight of dried activated carbon to the weight of dried eucalyptus. It was found that product yields from these runs were in the range of 50.7-68.8wt.%. From the analysis of variance (ANOVA), insignificant interaction terms ($P < 0.05$) in the full second-order polynomial was eliminated. The higher significance of corresponding coefficient has the larger F-test value and smaller P values. The model as shown in equation (2) was proposed. This reduced model was fitted between the responses represent specific surface area (Y) and the input variable of H_3PO_4 concentration (X_1), carbonizing temperature (X_2) and carbonizing time (X_3). The activated carbon with the highest specific surface area was obtained from using 2 M of H_3PO_4 solution and carbonization at $700^\circ C$ for 90 min. The predicted response value was $335.83\text{ m}^2/\text{g}$ closing to the experimental response value of $327\text{ m}^2/\text{g}$.

$$Y = 679.675 - 141.697X_1 - 1.180X_2 - 1.724X_3 + 73.565X_1^2 + 0.001X_2^2 + 0.010X_3^2 \quad (2)$$

It can be seen that the mathematical coefficients of X_1 was higher than others. This means that H_3PO_4 concentration had higher effect on the specific surface area of AC. The single factors (X_1 , X_2 and X_3) have negative sign, indicating that the specific surface area of produced AC (Y) decreased with increasing acid concentration, carbonizing temperature and time. Meanwhile, their second order terms (X_1^2 , X_2^2 and X_3^2) have positive sign, indicating positive effect on the response value (Y). Corresponding to the ANOVA of the RSM parameters (Table 4), the adequacy of the proposed model was assured by the high closely value of correlation coefficient ($R^2 = 0.9633$) and an adjusted correlation coefficient ($R_{adj}^2 = 0.9357$). Confirming an adequacy of the model fits, the F-value of this model (34.95) was clearly greater than the tabular F-value (3.58). Also, the proposed model with lack-of-fit (F-value of 3.09) revealing the lack of fit was insignificant relative to the pure error.

2. Response surface analysis for the specific surface area of produced activated carbon

To investigate the interactive effect of two variables on specific surface area of produced AC, the 3D response surfaces and contour plots obtained from reduced model (equation (2)) were drawn with one variable kept constant at their zero level and the other two varying within the experimental ranges as seen in Figure 1. These plots provide a method to predict the production efficiency of activated carbon with high specific surface area, for different values of the tested variables. So, the best response range can be obtained. The response contour and surface plot were developed as a function of H_3PO_4 concentration and carbonizing temperature, while the carbonizing time was kept constant at 90 min being a central level as shown in Figure 1(a) and (b). It can be seen that the specific surface area of produced AC increased with increasing temperature of carbonization. This can be attributed to the removal of volatile matter, organic, inorganic substance including tars from cross-linked framework generated by the treatment of phosphoric acid creating the pore structure which becomes more accessible when the chemical is removed by washing [4] Meanwhile, the specific surface area of produced AC decreased with increasing H_3PO_4 concentration from 0.5 to 1.35 M, and then increased continuously. Effect of increasing H_3PO_4 concentration on the specific surface area was enhanced with acid concentration exceeded than 1.35 M because the volume filling with acid ions and



various polyphosphates were increased. It can be described that these components quickly released from the particle surface during the carbonization, consequently, the gasification reaction moved faster resulting in larger specific surface area containing with higher pore volume and bigger pore size. Compared to the H_3PO_4 concentration used in impregnation step, the carbonizing temperature had little significant effect on specific surface area of derived-activated carbon. From this contour plot at constant carbonizing time of 90 min, it is noted that the maximum specific surface area of produced activated carbon for all concentrations presented at $700^\circ C$.

Figure 1(c) and (d) shows the contour and surface effect plot for the interaction of H_3PO_4 concentration and carbonizing time on the specific surface area of produced activated carbon at constant carbonizing temperature ($600^\circ C$). A slight changing of specific surface area could be observed with varying carbonizing time. High temperature accelerated the precursor degradation and evaporation of phosphate linkage leaving empty space previously occupied during carbonization at least 60 min, the specific surface area of produced activated carbon can be promoted at last. At high acid concentration, the increase of carbonizing time had stronger effect on specific surface area because high amount of phosphate linkage was formed by the interaction between the poly-phosphoric acid with the organic matter in biomass precursor. Thus, the carbonizing time had less effect on specific surface area of produced activated carbon compared to the H_3PO_4 concentration used in precursor impregnation step.

For precursor impregnation at the fixed H_3PO_4 concentration of 1.25 M, the contour and surface effect plot for the interaction of carbonizing temperature and time on the specific surface area of produced activated carbon are shown in Figure 1(e) and (f). Increasing of carbonizing temperature, the specific surface area of produced activated carbon was up to the optimum level with prolonging carbonization time to 120 min. This indicated that specific surface area was more dependent on carbonizing temperature than on time. At $700^\circ C$, the specific surface area was slightly reduced from carbonization for 76 to 102 min and clearly enhanced after carbonization longer than 112 min. An increase in the porosity and the total pore volume of activated carbon can be explained as the resulting from the completed evaporation of acid linkage and original matter under high carbonizing temperature with enough activating time. Thus, this can be concluded that the carbonizing time had less effect on specific surface area of produced activated carbon compared to the carbonizing temperature.

In order to obtain the condition for production of activated carbon with maximum specific surface area, numerical optimization with the function of desirability using the response optimizer in MINITAB (version 16) software was carried out. The experimental conditions with the highest composite desirability were selected to be verified. The optimum condition for preparation of activated carbon with high specific surface area was using H_3PO_4 concentration of 2 M for raw material impregnation following by carbonization at $700^\circ C$ for 120 min. The response predicted value was $351.101 \text{ m}^2/\text{g}$. To test the validity of predicted model (equation (2)), additional three runs (OP1, OP2 and OP3) were carried out under this optimum condition. The average experimental value of specific surface area of $358.707 \text{ m}^2/\text{g}$ was in good agreement with the predicted value from the proposed model. Therefore, the RSM was effective and reliable for optimizing the production condition of activated carbon with high specific surface area.



Through the process optimization, eucalyptus wood was proved to be a potential starting material for production of activated carbons with high surface area.

3. Characterization of produced activated carbons

From the model validation, OP1 activated carbon showed the higher specific surface area ($365.254\text{ m}^2/\text{g}$) than the others which prepared at the optimum condition as impregnation in 2M of H_3PO_4 solution and carbonization at 700°C for 120 min. However, this response was still lower than expectation of this study. Therefore, the addition tests were carried on for getting the preliminary data for the next work. The new investigation was emphasized on the precursor size, so the eucalyptus wood was milled using a high-speed rotary cutting mill and sieved to a particle size less than 10 mesh before immersion in H_3PO_4 solution. The activated carbon, named PT1, from this fine starting material was produced at the same condition to OP1. It had been revealed that PT1 had higher specific surface area ($559.956\text{ m}^2/\text{g}$) since the whole surface of carbon material could be totally interacted with acid ions during impregnation. These findings insisted that starting precursors with smaller particle size are superior in terms of their higher surface area interaction with activating agent. However, the specific surface area of obtained ACs from this study was still less than the related investigations. From ANOVA and RSM analysis, we have found that the acid concentration was the major effect on response. Also, the high BET surface areas and the total pore volumes of the activated carbon were reported by using concentrated H_3PO_4 solution (88%w/v) in impregnation step of Fox nutshell [3]. Therefore, we had conducted extra work by using stronger acid concentration in impregnation step for activated carbon production. We have found that using H_3PO_4 solution of 8M gave an increase of the specific surface area of produced activated carbon, named PT2, to $812.840\text{ m}^2/\text{g}$.

The SEM images of untreated char and AC samples derived from eucalyptus wood with H_3PO_4 are shown in Figure 2. Carbonization of eucalyptus wood at 700°C for 120 min gave less porosity structure of char with low specific surface area as evident from the SEM image given in Figure 2(a). Acid treatment of precursor before carbonization produced activated carbon with pores of different sizes and morphologies within the structure. From the optimum operating condition, OP1 with the connected pores allowing the obvious access to the micro porous within internal zones is shown in Figure 2 (b). This was attributed to the rupture of the biomass structure resulting from the acid impregnation stage and heating in the thermal stage. The images of PT1 and PT2 as shown in Figure 2(c) and (b), respectively, present the significant differences porous structure from OP1. This could be discussed as the larger specific surface area of precursors promotes more rapidly diffusion of activating agent into the pore structure, resulted from evaporation of H_3PO_4 during carbonization leaving empty spaced previously occupied by H_3PO_4 .

The surface of activated carbon composed of pores with a tunnel shape and fully developed honey-comb structure which opening holes was clearly observed. PT2 exhibited the well-developed uniform pores containing larger mesopores on the outside surface and less micropores on the wall resulting in higher specific surface area. The reason could be the deeply penetration of acid compound remaining intercalated in the internal structure of precursor surface during impregnation [5]. Throughout the activation, phosphoric acid reacted with the char and volatile matter and diffused quickly out the surfaces of particle. Therefore, using strong acid concentration led to the gasification of surface carbon atoms and the reduction of tars and other liquids which cause blocking of the pores and prevent the



growth of porous structure. This result approved that the concentration of the H_3PO_4 has strong effective in creating and developing porous structure of activated carbon corresponding to the other publications [6-8]. Table 5 shows the porous parameters of the eucalyptus wood, untreated char and its derived-ACs under different treatments. Herein, untreated char was prepared at the same carbonization condition to OP1 without pretreatment with H_3PO_4 activation. Up on the preparation condition as illustrated in Table 5, results revealed that ACs samples had better specific surface area, bigger average pore size and less microporosity than the untreated char. All ACs had mixed structure of microporous and mesoporous. OP1 presented mainly microporosity structure. Smaller particle size of starting material resulted in the developing of mesoporosity in produced ACs structure. Compared to untreated char and other ACs, PT2 had higher specific surface area (S_{BET}) up to $812.840\text{ m}^2/\text{g}$ with micropore volume (V_{mi}) and mesopore volume (V_{me}) of 0.128 and $0.306\text{ m}^3/\text{g}$, respectively. Its micropore surface area (S_{mi}) and mesopore surface area (S_{me}) was found to be 264.183 and $548.657\text{ m}^2/\text{g}$, respectively. These presented the large mesoporosity percentage based on surface area and pore volume which increased up to 67.499 and 70.507% , respectively. As discussed in the other works [3, 5, 9] the phosphoric acid and its derivatives (polyphosphoric acid) interact with the organic matter of biomass to form phosphate linkage serving the connected biopolymer crosslink generating the pore formation. These derivatives could fill a wide range of pore sizes and lead the evolution of large sized mesopores.

N_2 adsorption-desorption isotherms and pore size distribution of the untreated char and eucalyptus wood-derived ACs are shown in Figure 3(a) and (b), respectively. According to IUPAC classification, the isotherms of char and OP1 were typical type I adsorption isotherm, which dramatically increase at low relative pressure and reach to a horizontal plateau. These revealed that the char of untreated eucalyptus wood and activated carbon obtaining at the optimum condition (OP1) had predominantly microporous structure. From the plots of PT1 and PT2, the slope of these curves gradually increased, and the isotherms exhibited hysteresis loops. Thus, these activated carbons consisted of both micropores and mesopores which is the combination of Type I and Type IV according to IUPAC classification, the initial part of the isotherms was of Type I corresponds to adsorption in micropores. At intermediate and high relative pressures, the isotherms were type IV associating with monolayer-multilayer adsorption followed by capillary condensation in narrow slit-shaped pores. However, it was indicated that upon increasing acid concentration from 2 to 8M (precursor impregnation step), the isotherm plot moved toward a Type IV isotherm. This is commonly associated with the presence of mesoporosity, a common feature of type IV adsorption isotherms [10]. The greater fraction of mesoporosity was formed as proved by the mesopore volume percentage (Table 5).

Figure 3(b) compares the pore size distribution (PSD) of carbon products before and after the activation process with H_3PO_4 activation according to BJH method. The pores of the activated carbons are generally classified into three groups as micropore (diameter $< 2\text{ nm}$), mesopore ($2\text{ nm} < \text{diameter} < 50\text{ nm}$) and macropore (diameter $> 50\text{ nm}$) [4]. From this PSD graph, a less developed porous structure was observed for untreated char. The amount of micropores and the mesopores increased during H_3PO_4 activation drastically, indicating the micro pores might be collapsed into larger pores together with an initial mesopores had been developed from carbonization at 500 to 700°C . Moreover, the mesopore volume increased when the smaller particle size of precursor treated with H_3PO_4 of 8M, resulting in wider pore size distribution. The maxima of the distribution curves occur at 1.91 , 1.90 , 1.92 and 2.45



nm with different pore volumes (0.733, 0.291, 0.113, and 0.069 cm³/g) for PT2, PT1, OP1 and untreated char respectively. These results were consistent with textural properties and the isotherms as shown in Table 5 and Figure 3(a), respectively.

The thermal stabilities of eucalyptus wood and its derived-activated carbons were obtained using the technique of thermogravimetric analysis. The condition was heating rate of 10⁰C/min under nitrogen atmosphere. It was reported in weight percent remaining (TGA curve) and its corresponding first derivative as a function of reaction temperature (DTG curve). For TGA curves as seen in Figure 4, it can be divided into three stages of thermal degradation; dehydration, main devolatilization and the consolidation of the char structure. The DTG curves show an initial peak between 30 and 110⁰C, which corresponds to the evaporation of adsorbed water and light volatiles. Following this peak, the second stage covers a wide temperature range from 200 to 400⁰C, presenting two peaks in DTG curve. The first peak corresponds to the decomposition of hemicelluloses (280-320⁰C) causes the organic acid formation which accelerates the decomposition of polysaccharides. And the later was due to cellulose degradation in the range of 370-380⁰C [11]. Furthermore, the decomposition of lignin occurs at slower rate at the last stage indicating that the basic structure of the char residues has been formed and becomes almost constant. It had been observed that thermal degradation of prepared activated carbons (OP1, PT1 and PT2) started later in relation to eucalyptus wood and untreated char. It means the crystalline component was increased after H₃PO₄ activation leading to an increase of thermal stability. The proximate and ultimate analysis of untreated char and produced activated carbons are shown in Table 2. The OP1, PT1 and PT2 activated carbon had higher fixed carbon with lower content of ash and volatile matter than carbonized char without acid pretreatment. In addition, all produced activated carbons exhibited similar results in the elemental composition with higher carbon and lower oxygen content than untreated char and raw material. Moreover, chemical activation using phosphoric acid brought to a reduction in the H/C and O/C molar ratio from 1.49 and 0.69 in eucalyptus wood (Table2) to 1.03-1.06 and 0.39-0.41 in the selected activated carbons.

In order to provide further information, the chemical nature of functional groups on the untreated char and AC surface was analyzed by using FTIR with wavenumber of 4000 to 400 cm⁻¹ as shown in Figure 5. It can be observed that the activated carbon spectrum exhibits less adsorption bands than untreated char spectrum, indicating that some functional groups disappeared after acid activation and carbonization step. Although OP1 and PT1 were prepared via different conditions, there is a similarity in the absorption patterns, indicating that the surface functional groups do not exhibit significant differences except increasing the concentration of activating agent. The FTIR spectra of the activated carbons developed by phosphoric acid activation show absorption bands between 2300 and 2400 cm⁻¹. The peaks at 2315.69 cm⁻¹ for the PT2 may be assigned to carbon-oxygen bonds in ketene groups or the presence of -COOH functional groups. These bands are absent in the FTIR spectrum of the untreated char, OP1 and PT1. The bands were observed in the range 2260-2100cm⁻¹ for all samples are due to the C≡C bond. The band lies between 1650 to 2000 cm⁻¹ indicates C-H bending aromatic compound. The band between 1400 to 1750 cm⁻¹ exhibits carboxyl groups, quinones, ketones, lactones, diketone and keto-ether, and keto-enol. The presence of a band at



around 1690 cm^{-1} is observed. It may be due to the stretching vibrations of $\text{C}=\text{O}$ moieties in carboxylic acid groups, esters, lactones and quinines. The bands around 1600 cm^{-1} indicate the formation of carbonyl-containing groups and the aromatization of the precursor. An intense band at 1550 and 1650 cm^{-1} resulting from $\text{C}=\text{C}$ stretching vibrations in aromatic rings are enhanced by polar functional groups. All spectra shows band around 1560 cm^{-1} indicating oxidized carbons due to the combined stretching vibrations of $\text{C}=\text{O}$ group. Broadband at 1300 - 1000 cm^{-1} have been assigned to CO single bonds such as those in ethers, phenols, acids and esters. An intense band at 1500 - 950 cm^{-1} usually found in ACs obtained with phosphoric acid. This is due to phosphorous species as the stretching of hydrogen-bounded $\text{P}=\text{O}$, $\text{O}-\text{C}$ stretching vibrations in $\text{P}-\text{O}-\text{C}$ of aromatics and $\text{P}=\text{OOH}$, $\text{C}-\text{O}$ stretching in alcohols, carboxylic acids, esters, ethers. This observation was generally attributed to phosphorous and phosphorus carbonaceous compound in the phosphoric acid activated carbon [1]. These results suggested that phosphoric acid produced char oxidation and introducing oxygenated functionalities in the activated carbons. Increase concentration of phosphorous acid solution from 2 to 8M, the relative intensity of this broadband increased indicating more phosphorous-containing groups. In addition, the broadband at 1300 - 1000 cm^{-1} has been assigned to $\text{C}-\text{O}$ bonds such as those in ethers, phenols, acids and esters. Some bands also appeared in the range of 900 - 600 cm^{-1} , which were associated with the out-of-plane bending mode of the $\text{C}-\text{H}$ or $\text{O}-\text{H}$ group. Meanwhile, all carbon samples exhibit peaks of variable intensity in the region of 880 - 840 cm^{-1} relating to the out of plane bending vibrations of $\text{C}-\text{H}$ in aromatic rings with a large degree of substitution. The absorption band at 500 and 850 cm^{-1} , assigned to aromatics substituted by aliphatic groups, appears in the spectra of the AC. Also, with an increase in phosphorous concentration, band at 707.32 cm^{-1} appeared resulting from an increase in phosphorous-containing groups.

Discussion and Conclusions

The activated carbon with a well-developed porous structure was prepared from eucalyptus wood via impregnation in phosphoric acid following by carbonization. The effects of variables on the specific surface area like acid concentration, carbonizing temperature and time, also their interactions were determined by response surface methodology (Minitab16). ANOVA indicated that the proposed regression model based on Box-Behnken design has agreed with the experimental case with R^2 and R^2_{adj} correlation coefficients of 0.9725 and 0.9230 respectively. The concentration of phosphoric acid was the most strongly affects the specific surface area of porous activated carbon. The optimum condition for production of activated carbon with high surface area was phosphoric acid solution of 2M for impregnation step followed by carbonization at 700°C for 60 min. The experiment values were found to be agreed with the predicted value. Using the same carbonization condition after impregnation the smaller starting material in acid concentration of 8M gave of activated carbon with high surface area of $812.840\text{ m}^2/\text{g}$ containing of mainly mesopore structure. TGA and DTG results showed that all ACs had high thermal stability. Also, FTIR results confirmed the presence of phosphorous compounds in the porous activated carbon.



Acknowledgements

The project financial was supported by The Center of Knowledge Development of Rubber Tree in Northeast group (KDRN), Khon Kaen University, THAILAND.

References

1. Zhu GZ, Deng XL, Hou M, Sun K, Zhang YP, Li P, Liang FM. Comparative study on characterization and adsorption properties of activated carbons by phosphoric acid activation from corncob and its acid and alkaline hydrolysis residues. *Fuel Processing Technology*. 2016 Apr 1; 144:255-61.
2. Muniandy L, Adam F, Mohamed AR, Ng EP. The synthesis and characterization of high purity mixed microporous/mesoporous activated carbon from rice husk using chemical activation with NaOH and KOH. *Microporous and Mesoporous Materials*. 2014 Oct 1; 197:316-23.
3. Kumar A, Jena HM. Preparation and characterization of high surface area activated carbon from Fox nut (*Euryale ferox*) shell by chemical activation with H_3PO_4 . *Results in Physics*. 2016 Jan 1; 6:651-8.
4. Heidari A, Younesi H, Rashidi A, Ghoreyshi A. Adsorptive removal of CO_2 on highly microporous activated carbons prepared from Eucalyptus camaldulensis wood: Effect of chemical activation. *Journal of the Taiwan Institute of Chemical Engineers*. 2014 Mar 1;45(2):579-88.
5. Yakout SM, El-Deen GS. Characterization of activated carbon prepared by phosphoric acid activation of olive stones. *Arabian Journal of Chemistry*. 2016 Nov 1;9: S1155-62.
6. Wang B, Li Y, Si H, Chen H, Zhang M, Song T. Analysis of the Physical and Chemical Properties of Activated Carbons Based on Hullless Barley Straw and Plain Wheat Straw Obtained by H_3PO_4 Activation. *BioResources*. 2018 May 18;13(3):5204-12.
7. Duan X, Srinivasakannan C, Wang X, Wang F, Liu X. Synthesis of activated carbon fibers from cotton by microwave induced H_3PO_4 activation. *Journal of the Taiwan Institute of Chemical Engineers*. 2017 Jan 1; 70:374-81.
8. Valizadeh S, Younesi H, Bahramifar N. Preparation and Characterization of Activated Carbon from the Cones of Iranian Pine Trees (*Pinus eldarica*) by Chemical Activation with H_3PO_4 and Its Application for Removal of Sodium Dodecylbenzene Sulfonate Removal from Aqueous Solution. *Water Conservation Science and Engineering*. 2018:1-3.
9. Vunain E, Kenneth D, Biswick T. Synthesis and characterization of low-cost activated carbon prepared from Malawian baobab fruit shells by H_3PO_4 activation for removal of Cu (II) ions: equilibrium and kinetics studies. *Applied Water Science*. 2017 Dec 1;7(8):4301-19.
10. Kolodynska D, Krukowska J, Thomas P. Comparison of sorption and desorption studies of heavy metal ions from biochar and commercial active carbon. *Chemical Engineering Journal*. 2017 Jan 1; 307:353-63.
11. Chen Z, Zhu Q, Wang X, Xiao B, Liu S. Pyrolysis behaviors and kinetic studies on Eucalyptus residues using thermogravimetric analysis. *Energy Conversion and Management*. 2015 Nov 15; 105:251-9.

**Table 1** Experimental range and levels of independent variables

Independent variables	Symbols	Range and levels		
		Low level (-1)	Medium level (0)	High level (+1)
H_3PO_4 concentration (M)	X_1	0.5	1.25	2.0
Carbonizing Temperature (°C)	X_2	500	600	700
Carbonizing Time (min)	X_3	60	90	120

Table 2 Typical analysis of Eucalyptus wood, untreated char and produced activated carbons.

Condition	Raw	Untreated Char	OP1	PT1	PT2
Particle size	2-3 cm	2-3 cm	2-3 cm	10 mesh	10 mesh
H_3PO_4 (M)	None	None	2	2	8
Temperature (°C)	None	500	700	700	700
Time (min)	None	180	120	120	120
Proximate Analysis					
Moisture ^a	5.64	4.21	3.21	3.14	3.22
Volatile matter ^b	82.41	73.90	83.89	86.74	88.40
Fixed carbon ^b	16.61	25.32	15.64	12.88	11.25
Ash ^b	0.98	0.78	0.47	0.38	0.35
Ultimate Analysis^c					
C	52.4	58.59	60.55	61.11	61.43
H	0.3	5.41	5.33	5.31	5.29
O	42.2	34.52	32.95	32.5	32.23
N ^d	5.1	1.47		1.08	1.05
H/C molar ratio	1.49	1.11	1.06	1.04	1.03
O/C molar ratio	0.69	0.44	0.41	0.40	0.39
Empirical formula	$CH_{1.49}O_{0.69}$	$CH_{1.11}O_{0.44}$	$CH_{1.06}O_{0.41}$	$CH_{1.04}O_{0.40}$	$CH_{1.03}O_{0.39}$

^a As received basis; ^b Dry basis; ^c dry ash free basis. ^d Calculated by difference

Table 3 Box-Behnken experimental design and its value of response function.

Sample	H_3PO_4		Carbonizing Temperature (°C)	Carbonizing Time (min)	Surface area (m ² /g)	
	Concentration (M)				Experimental	Predicted
AC1	0.50		500	90	246.25	239.683
AC2	0.50		600	60	255.46	257.362
AC3	0.50		600	120	257.08	258.943
AC4	0.50		700	90	278.91	278.235
AC5	1.25		500	60	233.09	241.402
AC6	1.25		500	120	237.41	242.983
AC7	1.25		600	90	236.47	239.683
AC8	1.25		600	90	236.38	239.683
AC9	1.25		600	90	246.20	239.683
AC10	1.25		700	60	287.25	276.477
AC11	1.25		700	120	281.17	278.058
AC12	2.00		500	90	317.28	306.485
AC13	2.00		600	60	320.12	320.687
AC14	2.00		600	120	326.59	322.268
AC15	2.00		700	90	327.00	341.560

**Table 4** ANOVA for the adjusted specific surface area of activated carbon (reduced).

Source	DF	Seq SS	Adj SS	Mean square	F-value	Prob>F
Regression	6	17145.00	17145.40	2857.57	34.95	0.000
Linear	3	10485.60	3931.40	1310.48	16.03	0.001
X_1	1	8020.10	3603.30	3603.34	44.08	0.000
X_2	1	2460.50	356.00	355.97	4.35	0.070
X_3	1	5.00	270.80	270.83	3.31	0.106
square	3	6659.90	6659.90	2219.95	27.16	0.000
X_1^2	1	5958.00	6322.50	6322.49	77.34	0.000
X_2^2	1	419.10	471.10	471.13	5.76	0.043
X_3^2	1	282.80	282.80	282.75	3.46	0.100
Residual error	8	654.00	654.00	81.75		
Lack of fit	6	590.40	590.40	98.39	3.09	0.264
Pure error	2	63.70	63.70	31.83		

$R^2 = 0.9633$; $R_{adj}^2 = 0.9357$.

Table 5 BET results of eucalyptus wood char and its derived-activated carbons. (the operating conditions of untreated char, OP1, PT1 and PT2 are indicated in Table 2)

	Sample			
	Untreated Char	OP1	PT1	PT2
S_{BET} (specific surface area, m^2/g)	226.086	365.254	559.956	812.84
D_p (Average pore diameter, nm)	2.036	2.098	2.535	2.134
S_{mi} (microspore surface area, m^2/g)	179.801	221.014	294.709	264.183
S_{me} (mesospore surface area, m^2/g)	46.285	144.240	265.247	548.657
V_T (total pore volume, cm^3/g)	0.115	0.166	0.355	0.434
V_{mi} (micropore volume, cm^3/g)	0.089	0.108	0.145	0.128
V_{me} (mesopore volume, cm^3/g)	0.026	0.058	0.21	0.306
$S_{..}$ (%)	79.528	60.510	52.631	32.501
$S_{..}$ (%)	20.472	39.490	47.369	67.499
$V_{..}$ (%)	77.391	65.060	40.845	29.493
V_{me} (%)	22.609	34.940	59.155	70.507

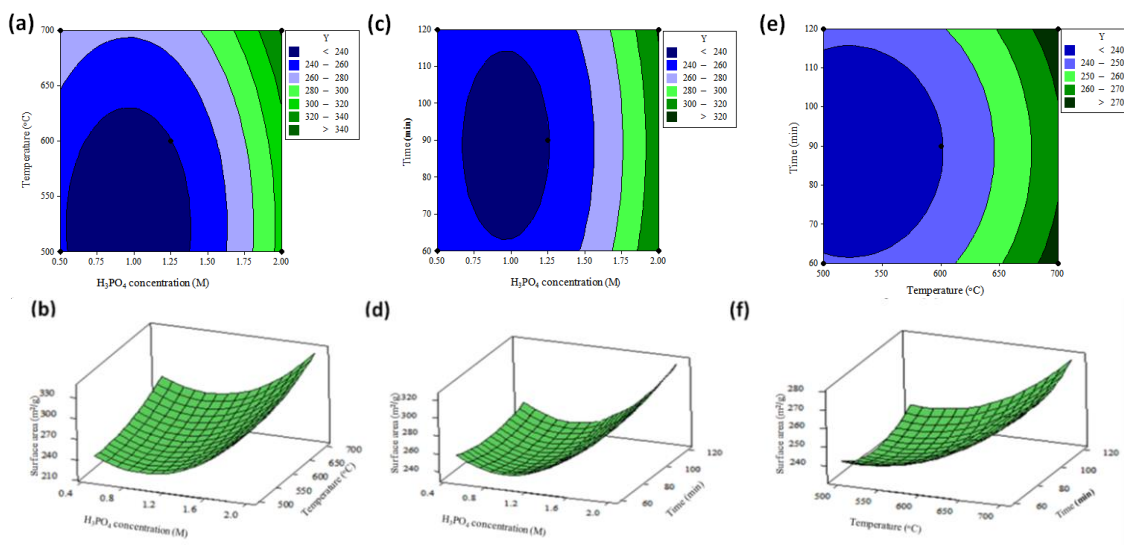


Figure 1 Contour and surface plot effects with two variables varied within the experimental ranges at constant value of 90 min (a and b), 600°C (c and d) and 1.25 M of H_3PO_4 (e and f).

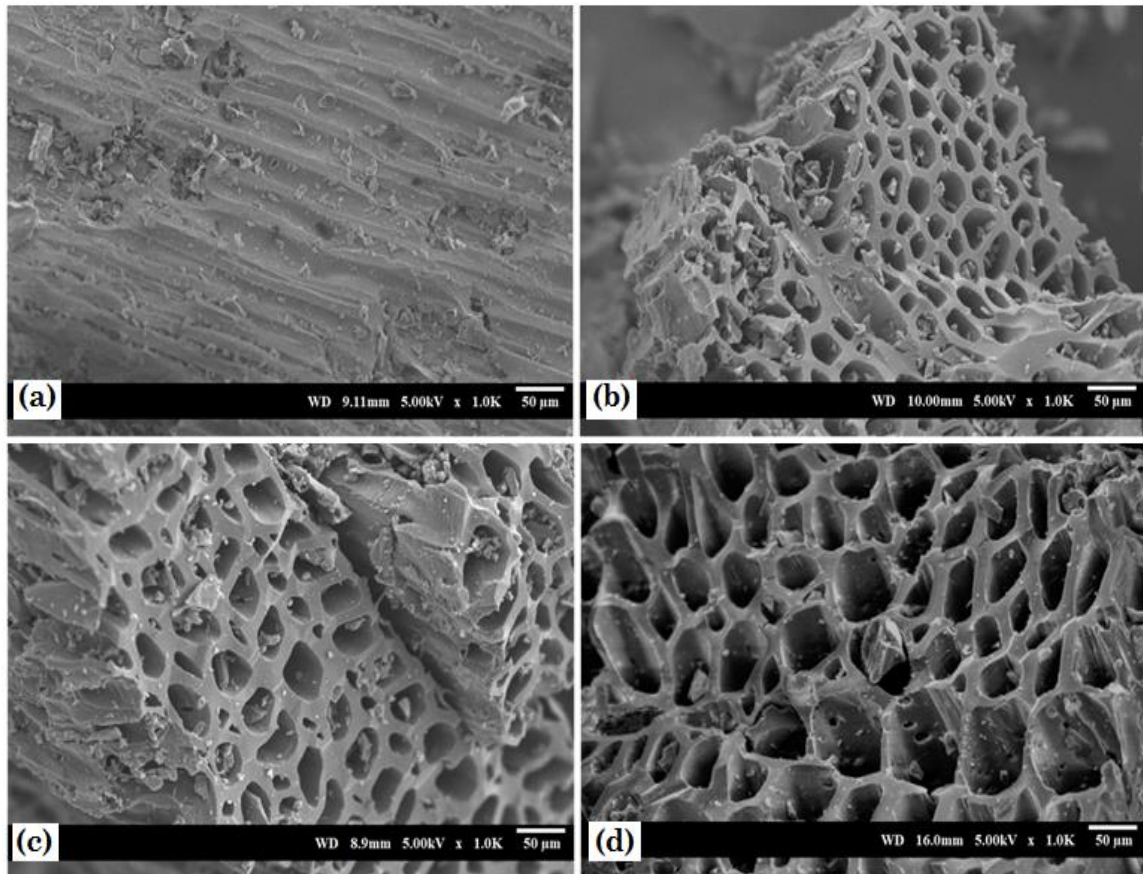


Figure 2 SEM images of: (a) untreated char and prepared AC of (b) OP1, (c) PT1 and (d) PT2

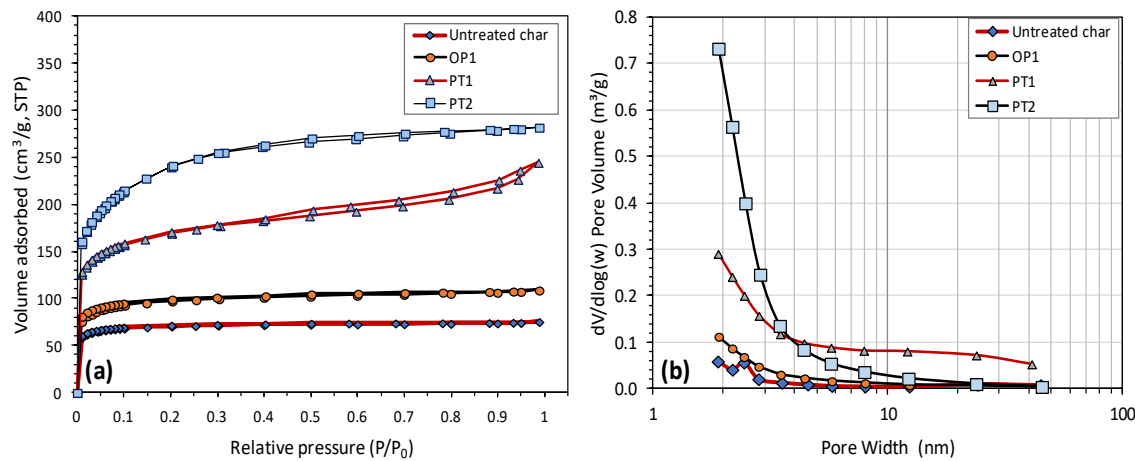


Figure 3 (a) N_2 adsorption/desorption isotherms and (b) pore size distribution of samples.

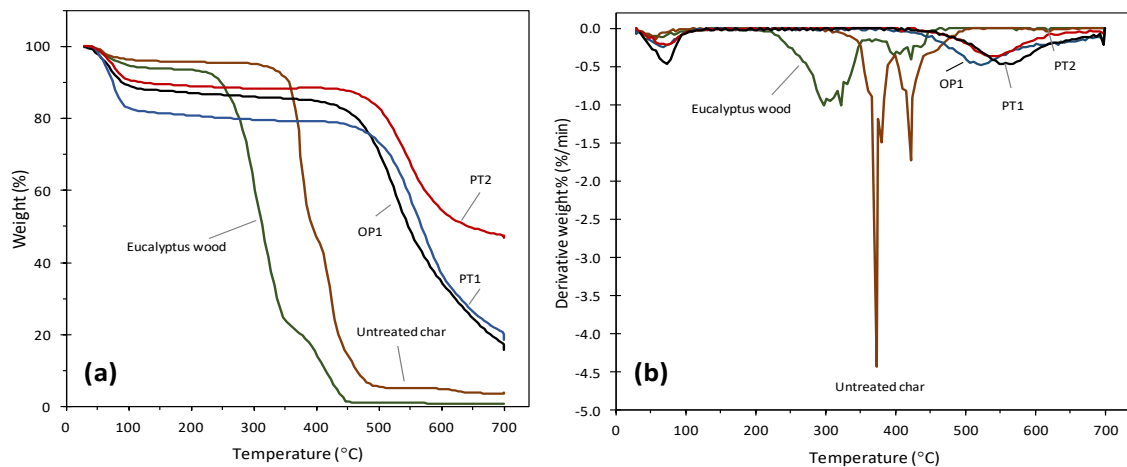


Figure 4 (a) TGA and (b) DTG thermograms for all selected samples.

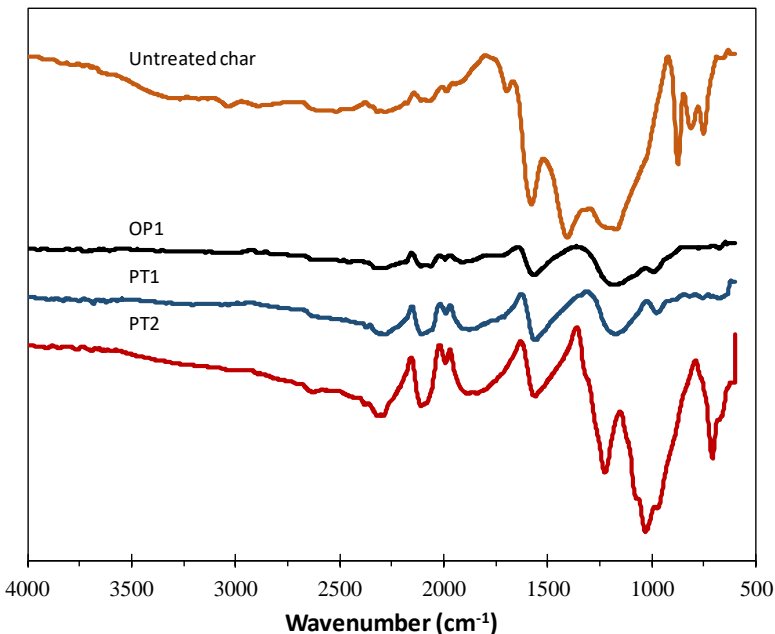


Figure 5 FTIR spectra for all selected samples.